

## High-loaded sub-6 nm Pt<sub>1</sub>Co<sub>1</sub> intermetallic compounds with high-efficient performance expression in PEMFCs

Qingqing Cheng<sup>a†</sup>, Shuai Yang<sup>b†</sup>, Cehuang Fu<sup>d</sup>, Liangliang Zou<sup>a\*</sup>, Zhiqing Zou<sup>a</sup>, Zheng Jiang<sup>b</sup>, Junliang Zhang<sup>d</sup> and Hui Yang<sup>a,c\*</sup>

<sup>a</sup> Dr. Q. Cheng, S. Yang, Dr. L. Zou, Dr. Z. Zou, Prof. Z. Jiang, Prof. H. Yang  
Shanghai Advanced Research Institute, Chinese Academy of Sciences, Shanghai 201210, P. R. China  
E-mail: yangh@sari.ac.cn; zoull@sari.ac.cn;

<sup>b</sup> S. Yang, Prof. Z. Jiang  
Shanghai Institute of Applied Physics, Chinese Academy of Sciences, Shanghai, 201204, China;

<sup>c</sup> Prof. H. Yang  
Ningbo Cotrun New Energy S&T Co., Ltd., Ningbo 315300 China;

<sup>d</sup> C. H. Fu, Prof. J. L. Zhang  
Institute of Fuel Cells  
Key Laboratory for Power Machinery and Engineering of MOE  
Shanghai Jiao Tong University  
800 Dongchuan Rd., Shanghai 200240, China

<sup>†</sup> Contributed equally to this work

### 1. Experimental section

#### 1.1. Synthesis of ultrafine Pt-NPs/C precursor

The carbon supported Pt-NPs was synthesized according to our previously reports. Specifically, the Pt carbonyl clusters were prepared by adding H<sub>2</sub>PtCl<sub>6</sub>·6H<sub>2</sub>O (purchased from Sigma-Aldrich), NaOH and CH<sub>3</sub>COONa (purchased from Sinopharm Chemical Reagent Co., Ltd.) with the mole ratio of 1: 4: 8 into 60 mL methanol solution kept at 55 °C for at least 8 h under a CO atmosphere. Thereafter, the pre-dispersed Vulcan XC-72R was quickly added into above solution under stirring for 8 h at 55 °C to control the Pt weight loading of 40 wt%. Then, the solvent was evaporated at 70 °C under N<sub>2</sub> purging and the obtained sample was slowly oxidized

at 0 °C for 2 days. Subsequently, the black precipitate was washed with DI-water for 3 times and dried in vacuum oven to obtain the Pt-NPs/C powder.

### **1.2. Fabrication of Co<sub>3</sub>O<sub>4</sub>/Pt-NPs/C precursor**

Co(NO<sub>3</sub>)<sub>2</sub>·6H<sub>2</sub>O (purchased from Sigma-Aldrich) and as-prepared Pt-NPs/C was dispersed into 50 mL DI-water with various Pt/Co mole ratio (3:1, 1:1 and 1:3) under ultrasonic for 2 h. Then, concentrated ammonia was added into above slurry to keep the pH around 9-10 and stirring for 12 h at 50 °C. After more times filtration, vacuum drying and grounding, the Co<sub>3</sub>O<sub>4</sub>/Pt-NPs/C precursor was achieved.

### **1.3. Preparation of Pt<sub>1</sub>Co<sub>1</sub>-IMC@Pt/C catalyst**

The as-prepared Co<sub>3</sub>O<sub>4</sub>/Pt-NPs/C precursor was subjected to heat-treatment under different temperature (T, T=500, 600, 700) for several hours (t, t=1, 2.5 and 4h) under 10% H<sub>2</sub>-90%Ar atmosphere with the heating rate of 7 °C min<sup>-1</sup>. After natural cooling to room temperature, the obtained powder was washed in warm 0.5 M H<sub>2</sub>SO<sub>4</sub> solution for 12 h to finally get the target samples, denoted as T-Pt<sub>1</sub>Co<sub>1</sub>-IMC@Pt/C-t.

## **2. Physical measurements**

Power X-ray diffraction (PXRD) were tested on Bruker AXS D8 ADVANCE powder X-ray diffractometer with a Cu K $\alpha$  ( $\lambda = 1.5418 \text{ \AA}$ ) radiation source, operating at 40 kV and 40 mA. Diffraction patterns were collected at a scanning rate of 2°·min<sup>-1</sup> and with a step size of 0.02°. TEM images were obtained by FEI Tecnai 30F microscope at an accelerating voltage of 200 kV. High Angle Annular Dark Field Scanning Transmission Electron Microscopy (HAADF-STEM) and X-ray energy dispersive spectrometry (XEDS) mapping were performed on a Double Cs-corrector FEI Titan Themis G2 60–300 microscope. X-ray photoelectron spectroscopy (XPS) was conducted using a Quantum 2000 Scanning ESCA Microprobe instrument with a monochromatic Al K $\alpha$

source (1486.6 eV). The binding energy (BE) scale was calibrated according to the C 1s peak (284.8 eV). The elemental compositions were calculated from the peak area ratios after corrected for the sensitivity factor of each element. The N1s spectra were deconvoluted by using a commercially available data fitting program (XPSPEAK41 software). The X-ray absorption near-edge structure spectra were collected on BL14W1 beamline of Shanghai Synchrotron Radiation Facility (SSRF) and analyzed with software of Iffeffit Athena.

### **3. Electrochemical characterization**

Cyclic voltammetry (CV) and linear sweep voltammetry (LSV) were performed on rotating disk electrode (RDE, 5 mm diameter) which was polished by  $\text{Al}_2\text{O}_3$  power, cleaned in  $\text{H}_2\text{O}$ /ethanol solution and dried naturally. Then the 20  $\mu\text{L}$  of prepared catalyst slurry with concentration of 1  $\mu\text{g}/\mu\text{L}$  was dropped on the glass electrode (GC) to lead the catalyst loading of 15  $\mu\text{g}_{\text{Pt}}\text{cm}^{-2}$ . Electrochemical tests were conducted on the CHI 730E equipped with a three-electrode system, using GC coated with catalyst as working electrode, GC as counter electrode and  $\text{Hg}/\text{Hg}_2\text{SO}_4$  as reference electrode. All the LSV tests were conducted in 0.1 M  $\text{HClO}_4$  with a rotation speed of 1600 rpm at a scan rate of 10  $\text{mVs}^{-1}$ . Accelerated durability test (ADT) was conducted by cycling the catalyst with the potentials range from 0.6 V to 1.1 V at a scan rate of 100  $\text{mVs}^{-1}$  under continuous purging  $\text{O}_2$  in electrolyte.

### **4. Membrane assembly electrode (MEA) preparation and single fuel cell testing**

For the PEMFCs, 8  $\mu\text{m}$  Gore membrane was selected as the proton exchange membrane. The MEAs with a  $2.5 \times 2.5 \text{ cm}^2$  active area were fabricated by catalyst coating membrane (CCM) method. The catalyst inks were prepared by dispersing 40 wt% Pt/C (anode) and as-prepared Pt1Co1-IMC@Pt/C (cathode) with 25 wt.% Nafion in isopropanol/ $\text{H}_2\text{O}$  solution under ultrasonic for 3 h. The anode consisted of Pt/C with a metal loading of 0.1  $\text{mg cm}^{-2}$ . The cathode consisted of Pt1Co1-IMC@Pt/C catalysts with the Pt loading of 0.2  $\text{mg cm}^{-2}$ . The performance of PEMFCs were measured by polarization test on Arbin Fuel Cell Testing System (Arbin Instrument Inc., USA)

and the polarization data was recorded per 2 min. The as-prepared MEAs were activated and tested in a PEMFC testing setup by purging H<sub>2</sub> into the anode with the flow rate of 1 standard liter per minute (slpm) and O<sub>2</sub> or air into the cathode with flow rate of 0.4 slpm and 1.5 slpm. The testing temperature was controlled at 80 °C with 100 RH% and the back-pressure was fixed at 1 bar. The high-frequency resistance of MEA was recorded using battery resistance meter.

## 5. Density functional theory calculation

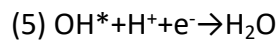
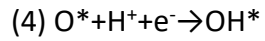
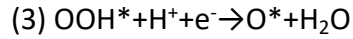
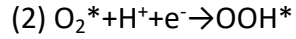
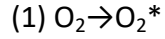
All calculations are performed by Density Functional Theory (DFT) on *Vienna Ab initio Simulation Package* (VASP). The ion-electron interaction and the exchange-correlation errors are described by projector augmented wave (PAW) method and Perdew-Burke-Ernzerhof (PBE) functional. the cutoff energy, residual energy and force are set as 500 eV, 10<sup>-6</sup> eV/atom and 0.02 eV/Å.

There are three kinds of 5-layer-slab models are used in our calculation to study the effect of Co, which consist of (111) facet and marked as pure-Pt, PtCo. Pure-Pt model contains 20 Pt atoms without strain effect. PtCo model is consist of PtCo core (1:1) and Pt skin according to the fact that Co atom would be etched after acid-washing and ORR process. The top two layers are relaxed. A vacuum slab of 15 Å and a Monkhorst-Pack grid of 7x7x1 are applied. It is well known that the content of Co-Co bond would increase when PtCo alloy become disordered. To understand the anti-oxidization of Co atoms in disordered and ordered PtCo alloys, the adsorption energies of O atom on two kinds of 4x4 slab models (Figure S16) are calculated with a Monkhorst-Pack grid of 4x4x1 as:

$$G_{O^*} = G_{ad} - G_{O_2} - G_{slab} - 2(G_{H^+} + G_{e^-}) + G_{H_2O}$$

Where  $G_{ad}$ ,  $G_{O_2}$ ,  $G_{slab}$ ,  $G_{H^+}$ ,  $G_{e^-}$ ,  $G_{H_2O}$  are free energies of slab with adsorbed O atom, clean slab, H<sup>+</sup>, e<sup>-</sup> and H<sub>2</sub>O.

The oxygen reduction reaction (ORR) is performed as a four-electron reaction in an acid environment:



The free energy is given as:

$$G = E_{\text{DFT}} + \text{ZPE} - TS - neU$$

where  $E$  is the DFT energy,  $\text{ZPE}$  is the zero-point energy which is equal to  $\sum(h\nu_i/2)$  ( $h$  is the Planck constant and  $\nu_i$  is the vibrational frequency),  $T$  is the temperature (298.15 K),  $S$  is the entropy of the structure,  $n$  is the number of electrons transferred in elementary reaction,  $e$  is the charge constant and  $U$  is the potential.

The free energy of ( $\text{H}^+ + \text{e}^-$ ) is defined as half of that of  $\text{H}_2$  on the standard condition ( $U=0$ ,  $\text{pH}=0$ ).  $\text{H}_2$  and  $\text{H}_2\text{O}$  are calculated with DFT.  $G_{\text{H}_2\text{O}(l)} = G_{\text{H}_2\text{O}(g)} + RT \times \ln(P/P_0)$  is used to get the energy of  $\text{H}_2\text{O}$ , where  $R$  is gas constant,  $P_0=1$  bar and  $P=0.035$  bar. The energy of  $\text{O}_2$  is calculated according to the energy released (4.92 eV) in  $4\text{e}^-$  ORR process.

$\Delta G_i$  ( $i=1, 2, 3, 4, 5$ ) is calculated as the energy difference between elementary reaction. And the activity of catalyst models can be described by onset potential as:

$$U_{\text{onset}} = \max \Delta G_i / e$$

## Supplementary figures

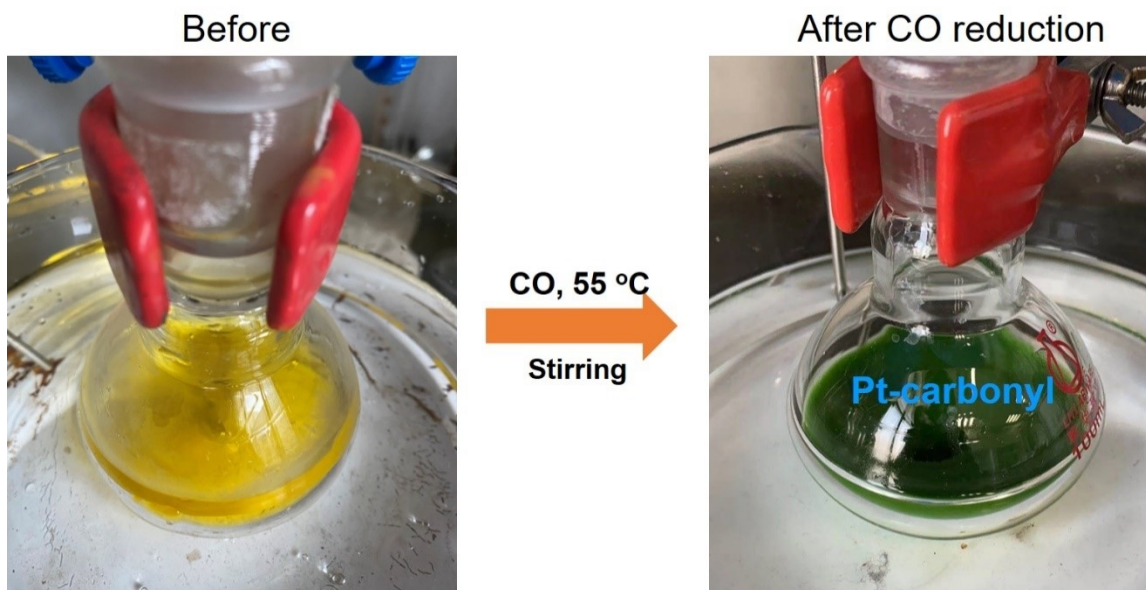


Figure S1. Photographs of preparation for Pt-carbonyl clusters

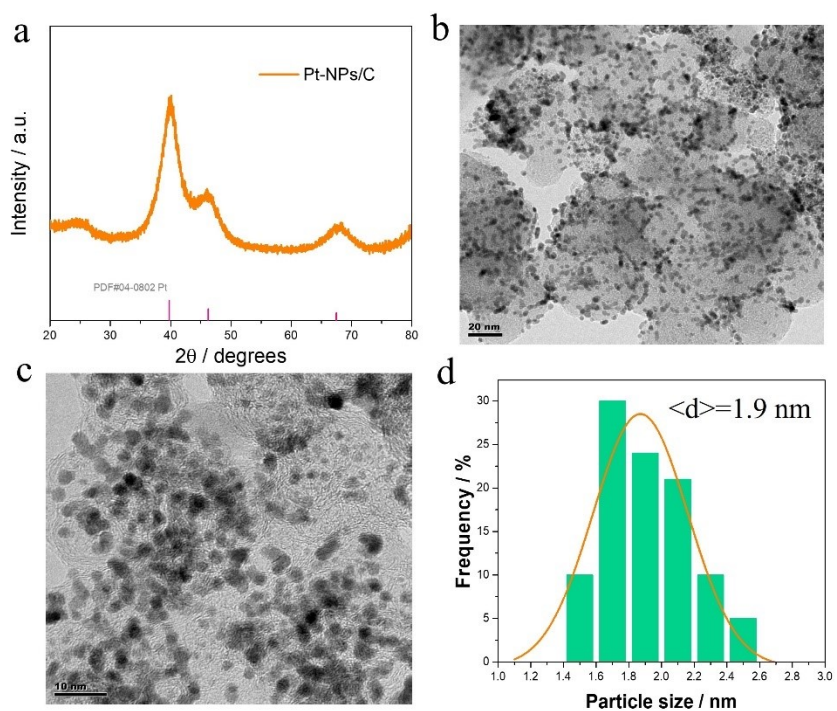


Figure S2. (a) XRD, (b) TEM (c) high-magnified TEM (d) size distribution histogram of as-prepared Pt-NPs/C precursor.

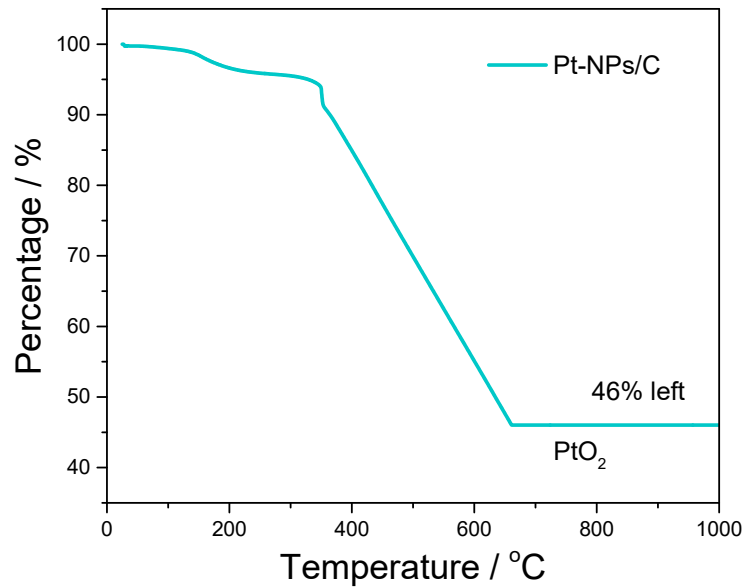


Figure S3. TG curve of Pt-NPs/C under O<sub>2</sub> atmosphere.

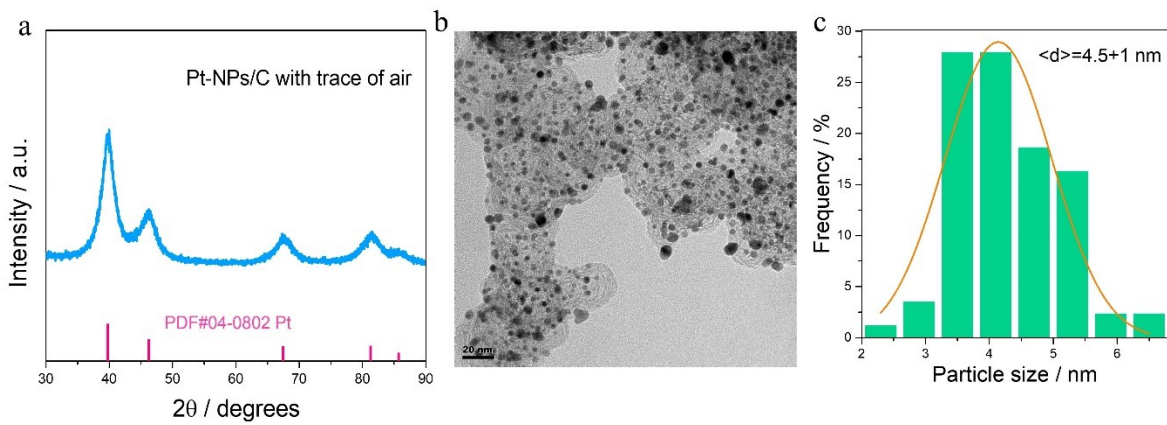


Figure S4. (a) XRD pattern (b) TEM image and (c) size distribution histogram of Pt-NPs/C precursor prepared with trace of air.

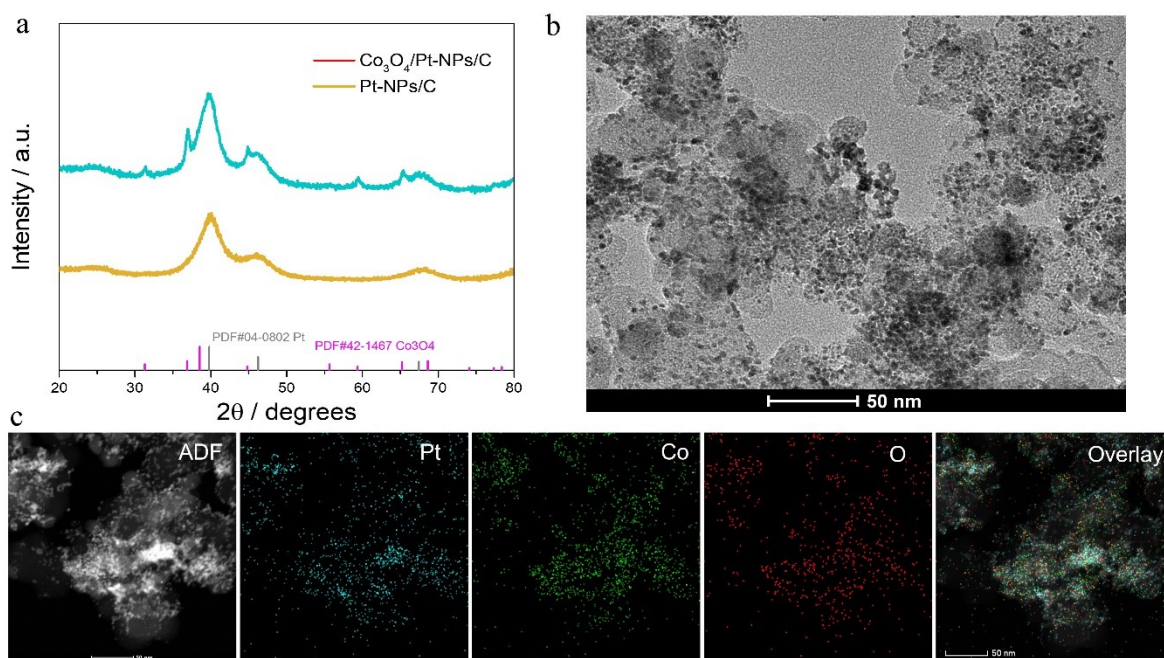


Figure S5. (a) XRD pattern (b) TEM image (c) EDS-mapping of Co<sub>3</sub>O<sub>4</sub>/Pt-NPs/C precursor.

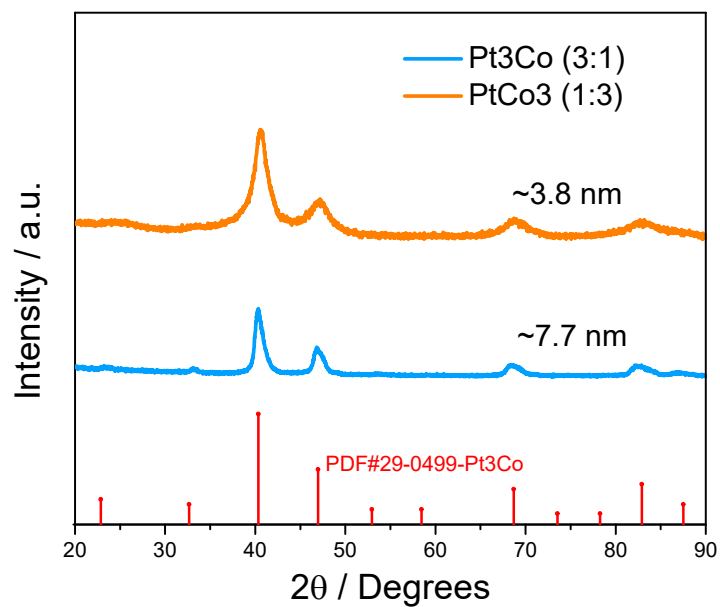


Figure S6. XRD patterns of PtCo/C catalyst prepared with different Pt/Co feeding ratio at 700 °C for 2.5 h.

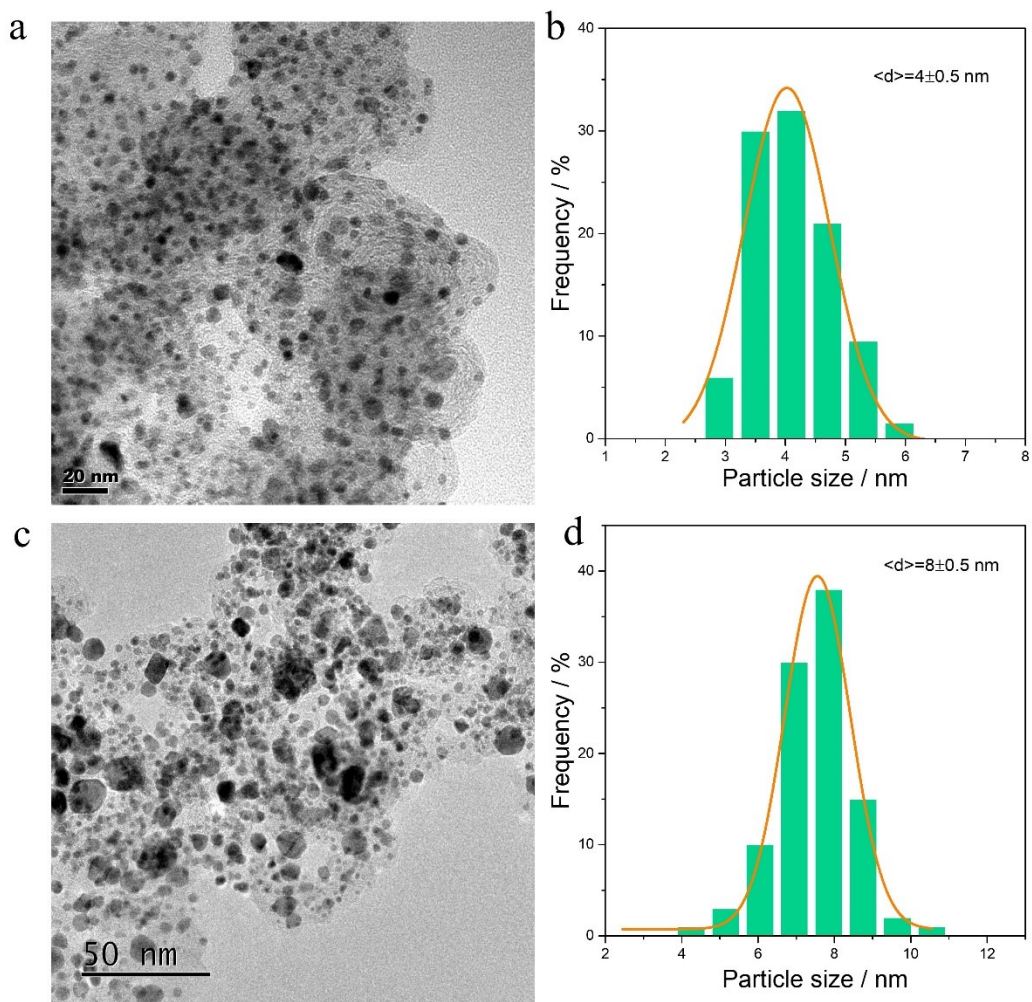


Figure S7. TEM images and size distribution histogram for (a, b) PtCo/C (1:3) and (c, d) PtCo/C (3:1) contrast catalysts.

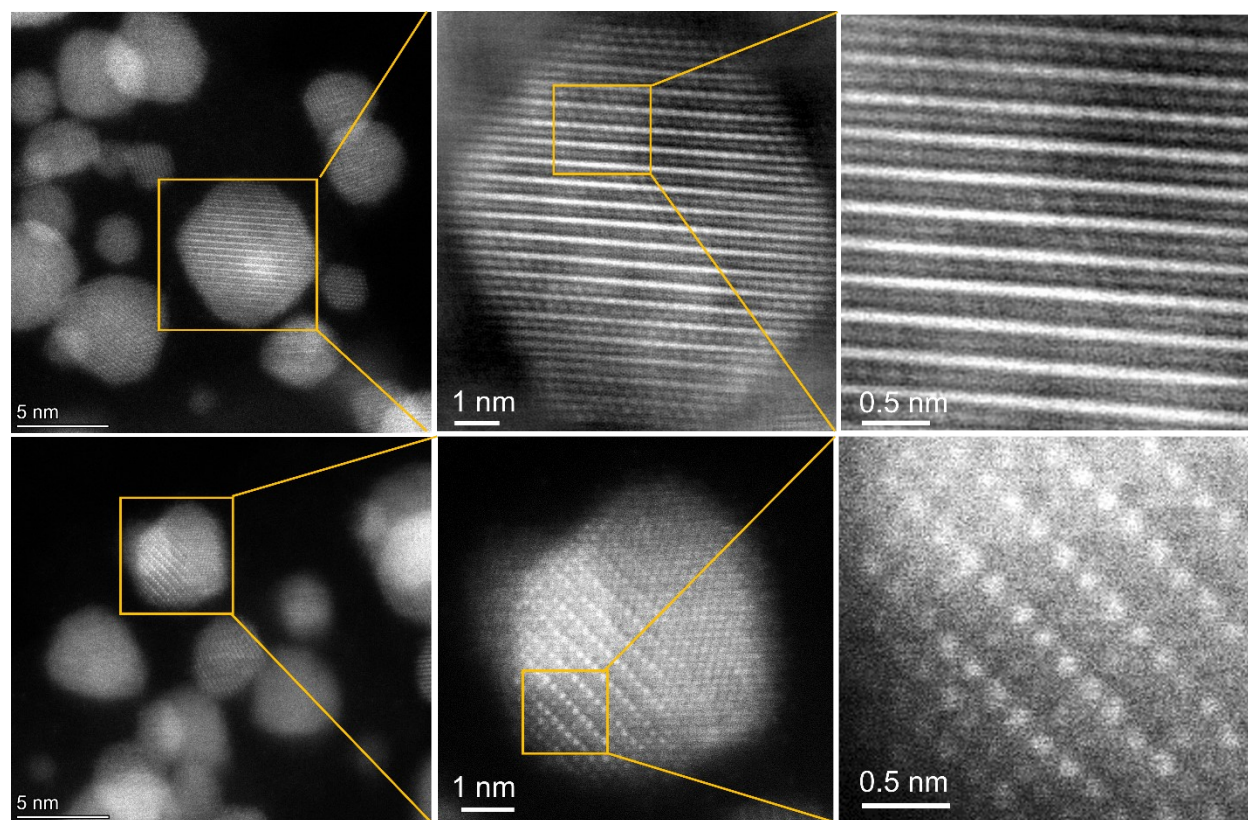


Figure S8. Atomic resolution STEM images for as-prepared 700-Pt1Co1-IMC@Pt/C-2.5 catalyst at different locations.

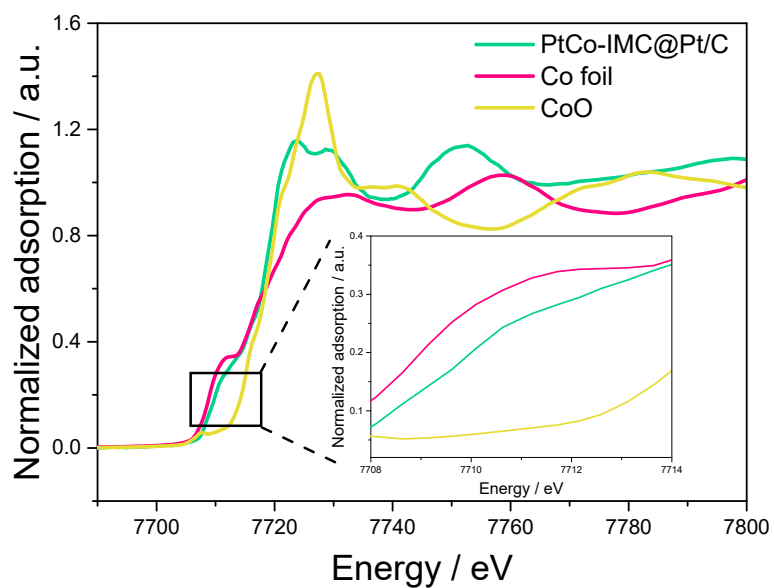


Figure S9. Co K-edge XANES spectra for the Pt1Co1-IMC@Pt, Co foil and CoO samples

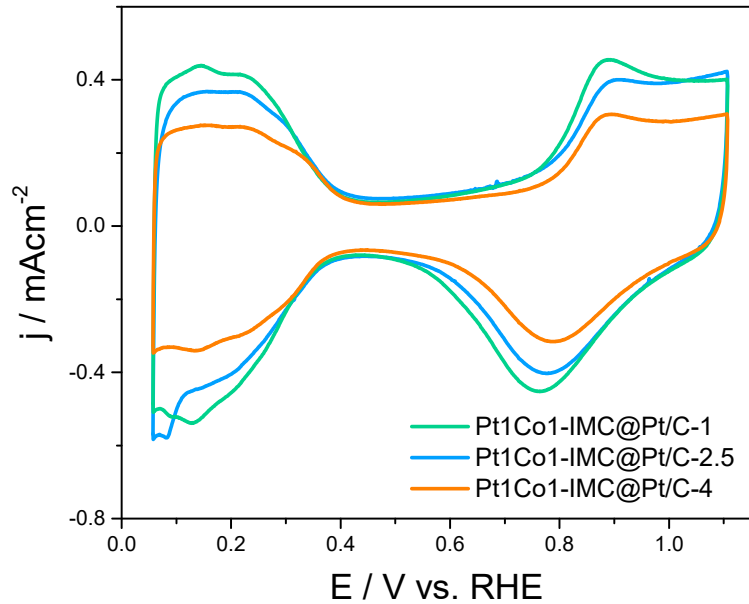


Figure S10. CV curves on Pt1Co1-IMC/C catalysts prepared for various annealing times in  $N_2$ -saturated 0.1 M  $HClO_4$  solution with scan rate of  $50 \text{ mVs}^{-1}$ .

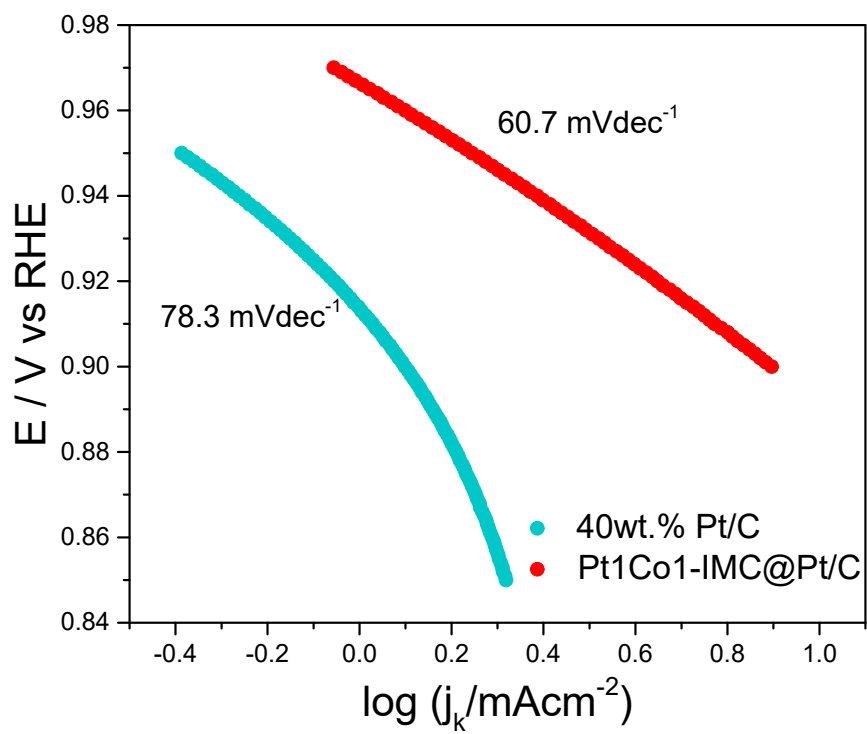


Figure S11. Tafel plots for Pt1Co1-IMC@Pt/C and commercial Pt/C catalysts

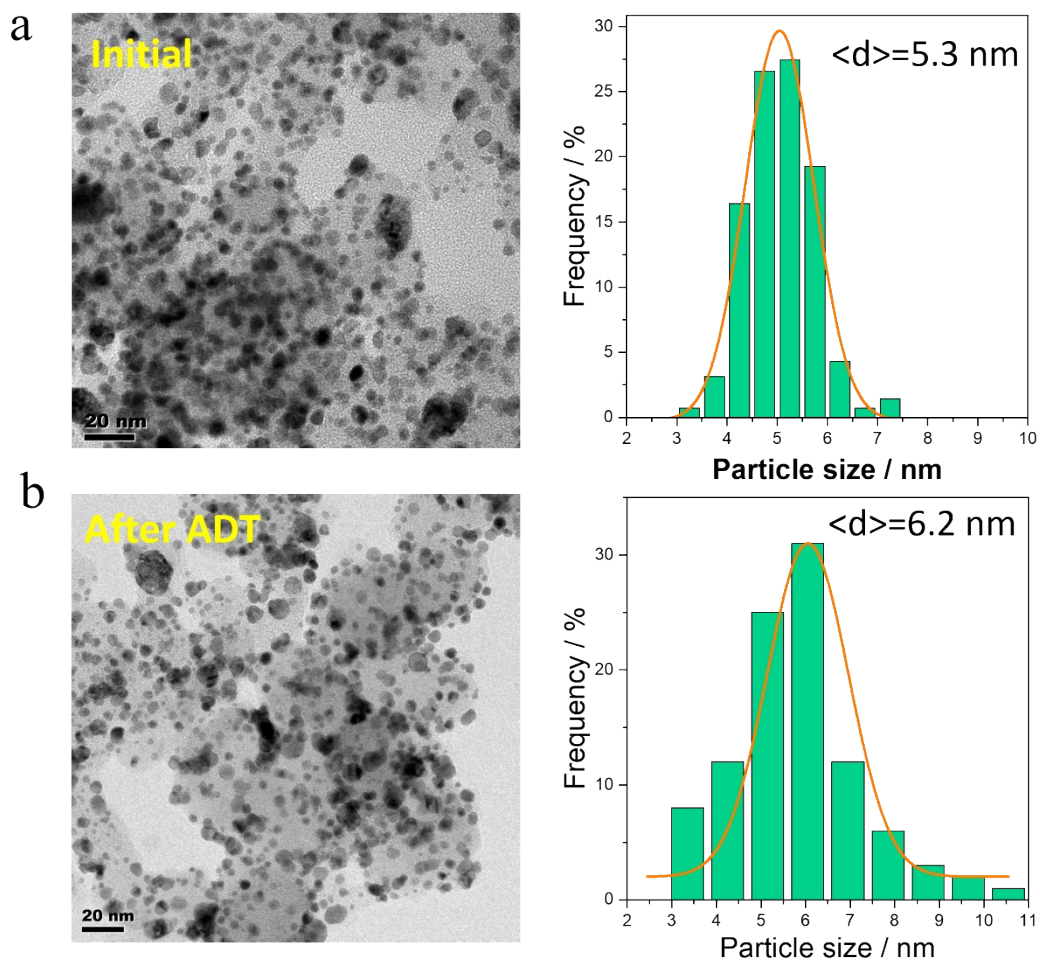


Figure S12. TEM images and corresponding size distribution of Pt<sub>1</sub>Co<sub>1</sub>-IMC@Pt/C (a) before and (b) after ADT.

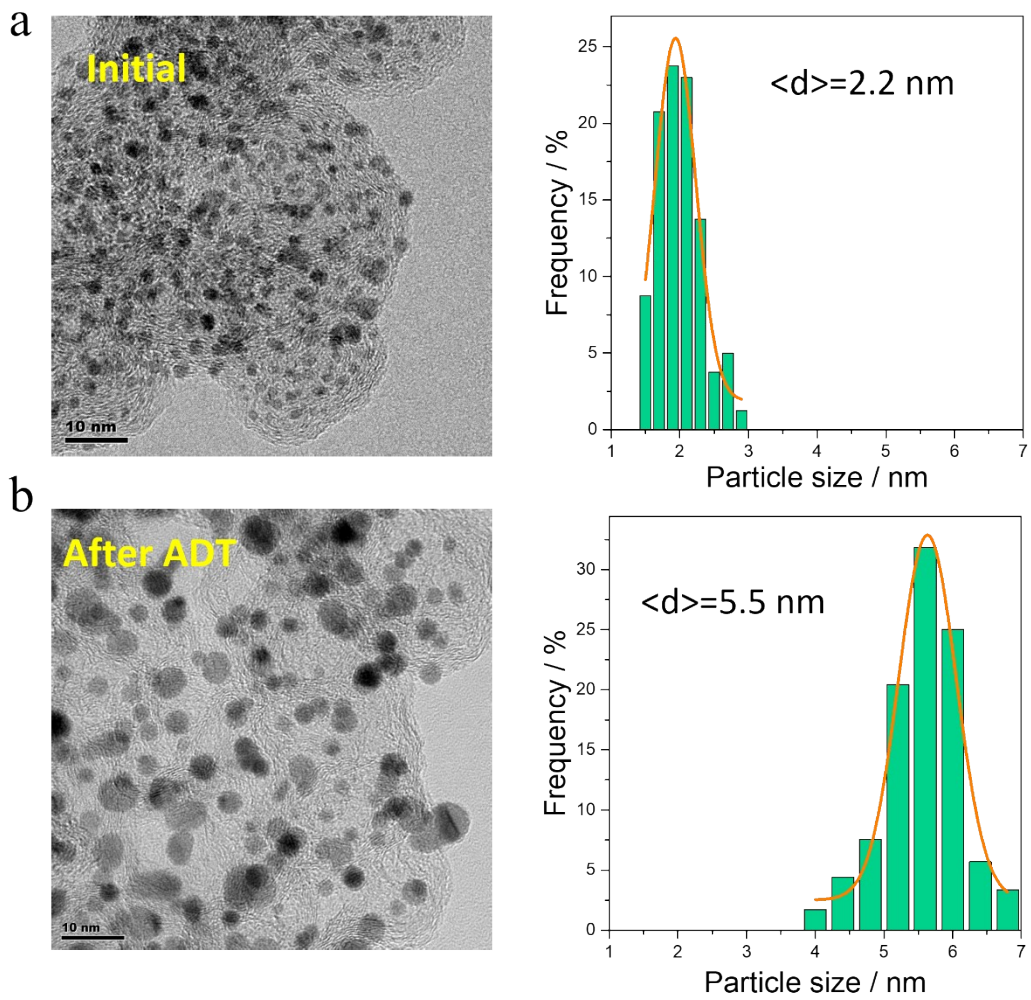


Figure S13. TEM images and corresponding size distribution of commercial Pt/C (a) before and (b) after ADT.

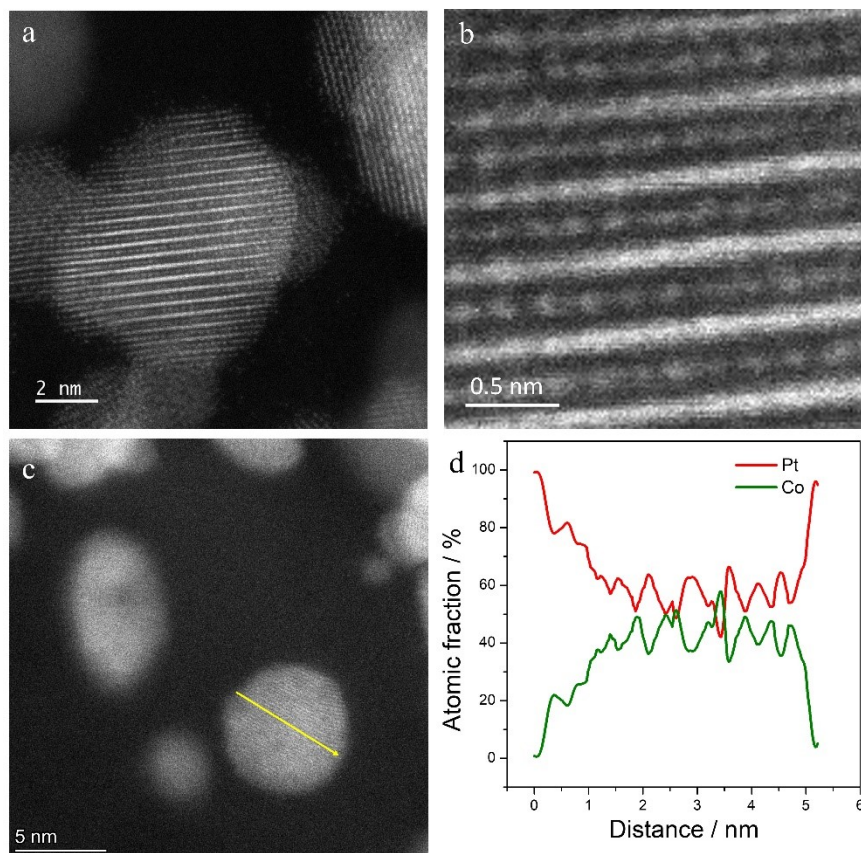


Figure S14. (a, b) STEM images (c, d) EDS line-profile for Pt1Co1-IMC@Pt/C catalyst after ADT

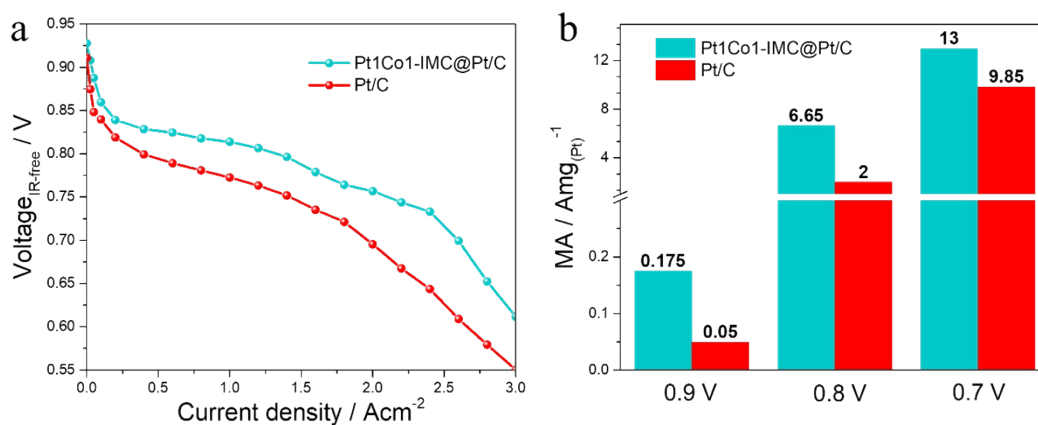


Figure S15. (a) H<sub>2</sub>-Air polarization curves corrected by high-frequency resistance; (b) Mass activities for Pt1Co1-IMC@Pt/C and commercial Pt/C at various voltages.

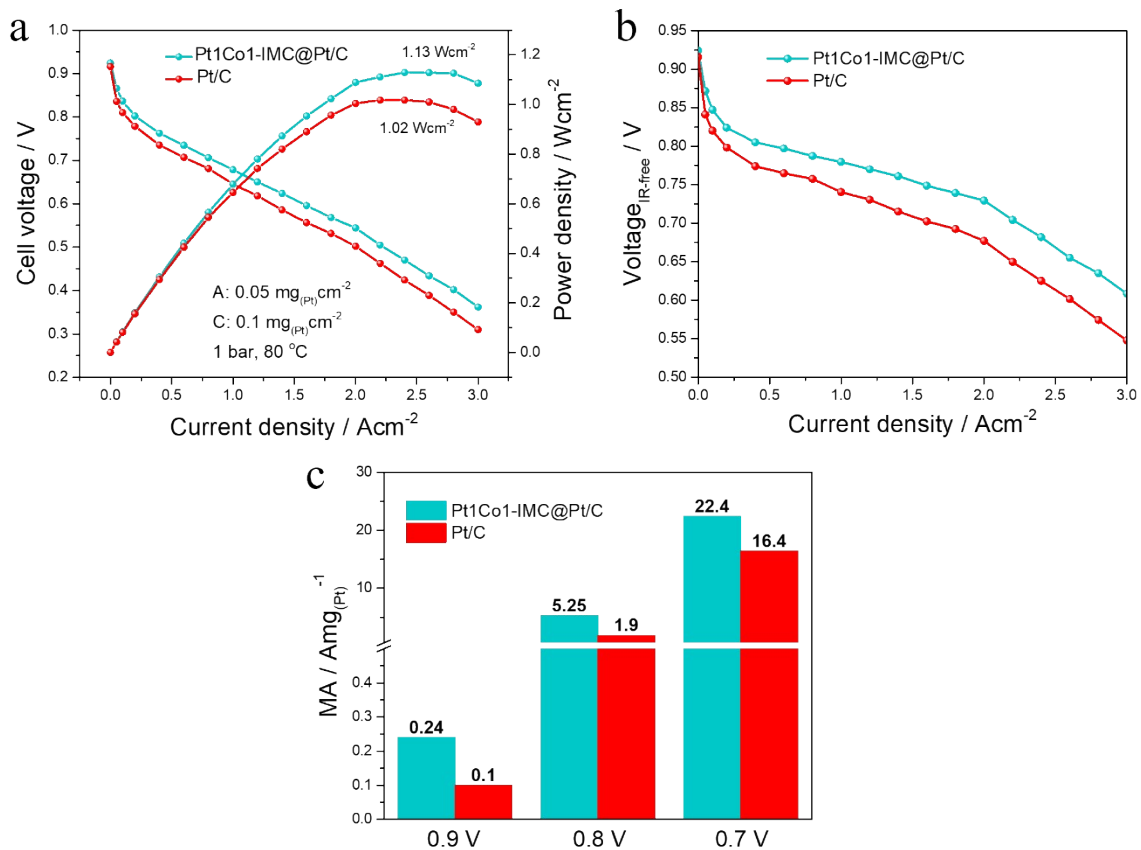


Figure S16. (a) Steady-state polarization curves of MEAs prepared by using Pt1Co1-IMC@Pt/C and commercial 40 wt.% Pt/C as cathode catalysts with low Pt usage. (A: 0.05 mg<sub>(Pt)</sub>cm<sup>-2</sup>, C: 0.1 mg<sub>(Pt)</sub>cm<sup>-2</sup>) under H<sub>2</sub>-air condition; (b) IR-free polarization curves and (c) corresponding MAs at various voltages.

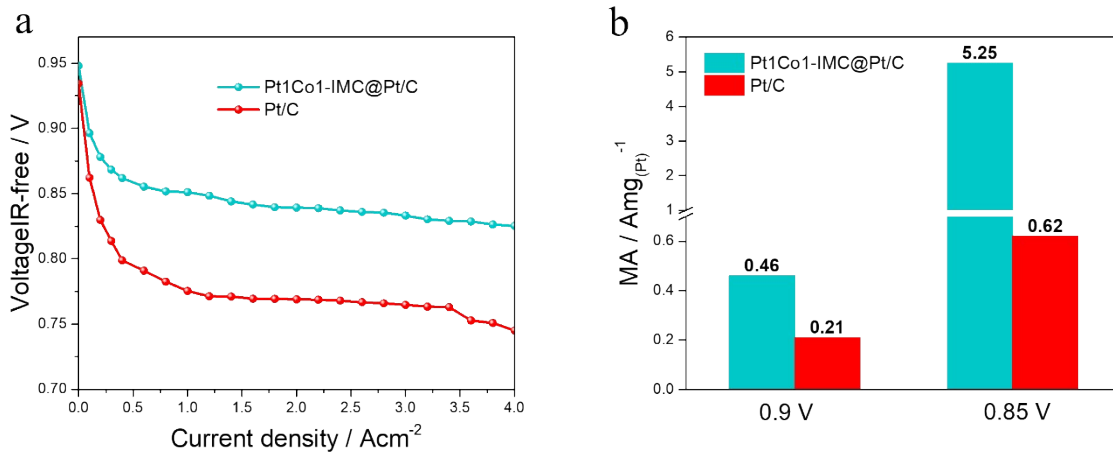


Figure S17. (a) comparison of IR-free polarization curves for Pt1Co1-IMC@Pt/C and Pt/C catalysts under H<sub>2</sub>-O<sub>2</sub> condition; (c) Mass activities for Pt1Co1-IMC@Pt and commercial Pt/C at 0.9 V and 0.85 V, respectively.

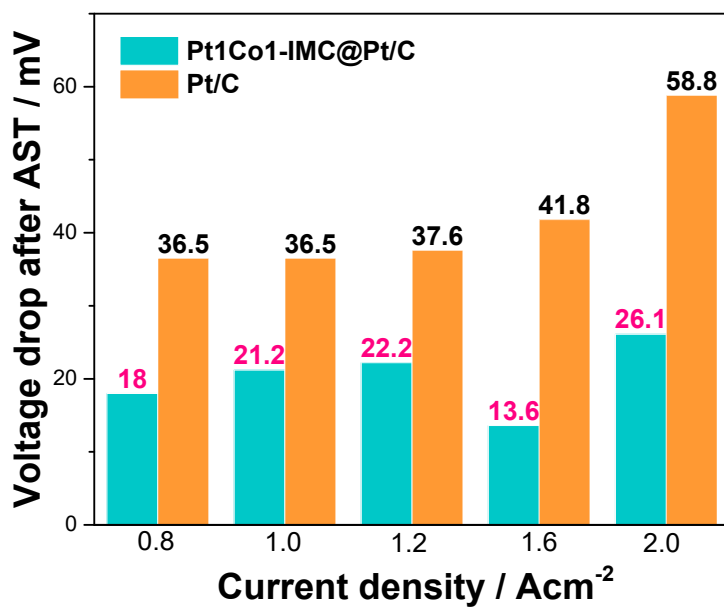


Figure S18. Voltage drops for Pt1Co1-IMC@Pt/C and Pt/C after AST at various current densities.

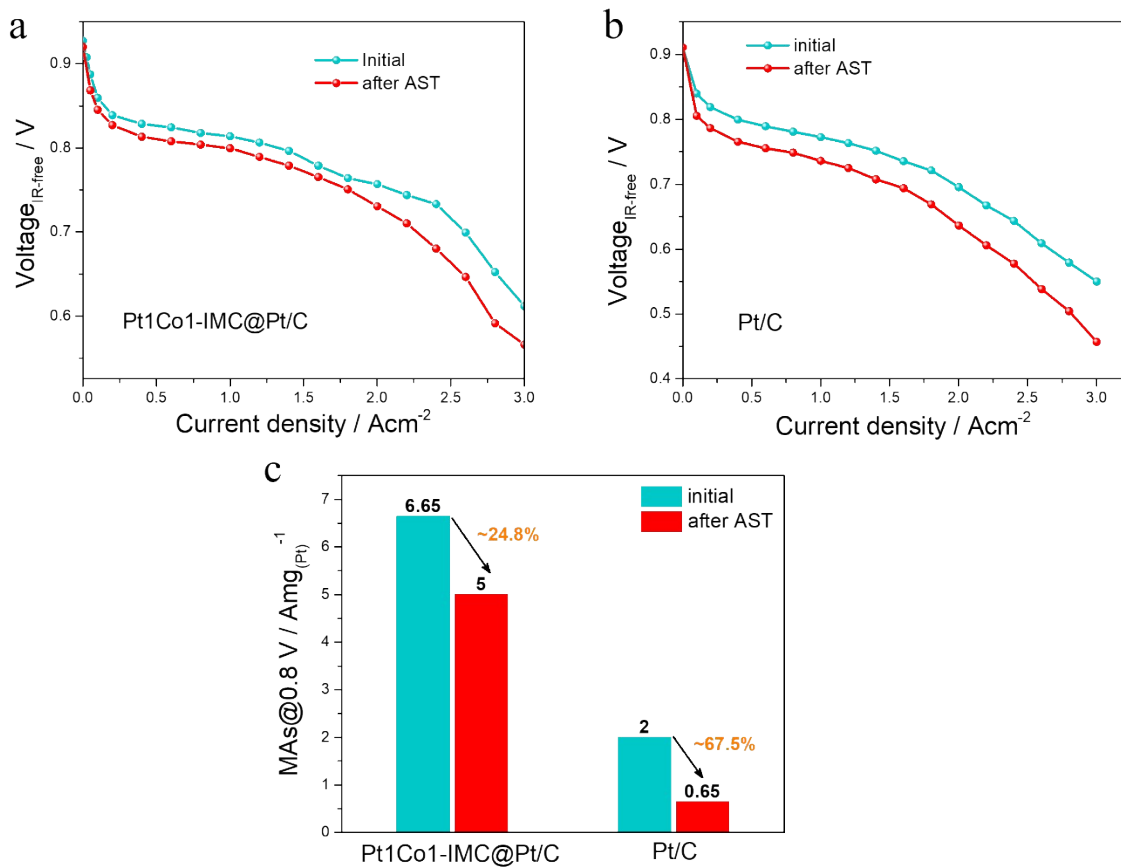


Figure S19. (a, b) HFR-corrected I-V curves for Pt1Co1-IMC@Pt/C and commercial Pt/C before and after AST (c) corresponding MA degradation comparison at voltage of 0.8 V<sub>(IR-free)</sub>.

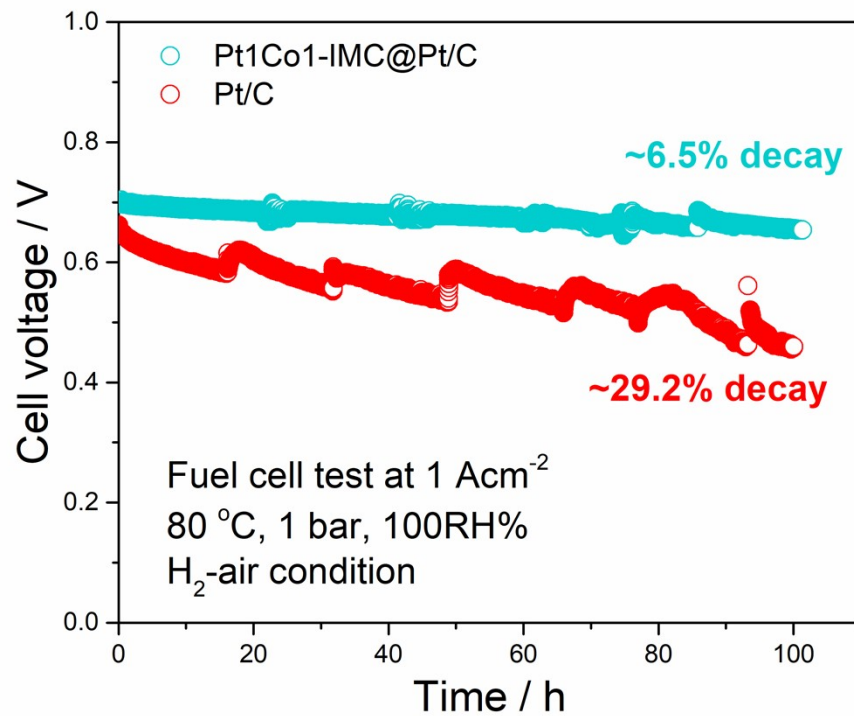


Figure S20. Long-term stability test for H<sub>2</sub>-air integrated with Pt1Co1-IMC@Pt/C and commercial catalyst Pt/C catalysts at a constant current density of 1 Acm<sup>-2</sup>.

**Table S1.** ICP results for various samples.

Sample	Mass / mg	Volume / mL	Pt / mgL <sup>-1</sup>	Co / mgL <sup>-1</sup>	Atom ratio (Pt : Co)
Pt-NPs/C	14	500	11.45		
Pt1Co1-IMC/C-1	14	500	10.60	1.59	67:33
Pt1Co1-IMC/C-2.5	13	500	9.53	2.11	57:43
Pt1Co1-IMC/C-4	10	500	6.44	1.68	53:47

**Table S2.** The fitting parameters of Pt L-edge and Co K-edge for various samples

Sample	Shell	N <sup>[a]</sup>	R <sup>[b]</sup> (Å)	$\Delta E_0$ <sup>[c]</sup> (eV)	$\sigma^{2[d]}$ ( $10^{-3}\text{\AA}^2$ )	R-factor
Pt-foil	Pt-Pt	12	2.76±0.00	7.3±0.4	4.6±0.2	0.002
Co-foil	Co-Co	12	2.49±0.00	7.4±0.4	6.2±0.2	0.001
Pt/Co	Pt-Co	4.7	2.64 ± 0.01	5.2 ± 1.2	6.9 ± 0.1	0.003
	Pt-Pt	5.8	2.69 ± 0.01	2.1 ± 1.2	5.4 ± 0.1	
	Co-O/N	1.0	2.10 ± 0.04	10.0 ± 0.0	10	
Co/Pt	Co-Co	3.2	2.61±0.01	-6.7±2.8	8.1±2.0	0.009
	Co-Pt	4.0	2.65±0.01	-3.8±2.1	5.0±1.4	

[a] coordination numbers; [b] the internal atomic distance; [c] the edge-energy shift. [d] Debye-Waller factor;

**Table S3.** The performance of H<sub>2</sub>-air PEMFCs with advanced Pt-based catalysts as cathode.

Sample	Test condition	Peak power density / mWcm <sup>-2</sup>	Current density@0.65V / Acm <sup>-2</sup>	Reference
Pt1Co1-IMC@Pt/C	Cathode: 0.2 mgcm <sup>-2</sup> , BP <sup>[a]</sup> : 100kPa, 80 °C, 100%RH	1.23	1.45	This work
Pt1Co1-IMC@Pt/C	Cathode: 0.1 mgcm <sup>-2</sup> , BP: 100kPa, 80 °C, 100%RH	1.13	1.20	This work
P-Pt/C	Cathode: 0.15 mgcm <sup>-2</sup> , BP: 50kPa, 80 °C, 100%RH	1.06	~1.20	1
Coplanar Pt/C	Cathode: 0.1 mgcm <sup>-2</sup> , BP: 150kPa, 80 °C, 100%RH	0.553	~0.71	2
Fine grain PtFe/C	0.225 mgcm <sup>-2</sup> , BP: 150kPa, 80 °C, 100%RH	~0.59	0.62	3
L10-FePt/Pt	0.101 mgcm <sup>-2</sup> , BP: 150kPa, 80 °C, 100%RH	~0.6	~0.82	4
Pt/40Co-NC-900	0.13 mgcm <sup>-2</sup> , BP: 150kPa, 80 °C, 100%RH	~0.7	~1.01	5
PtCo/NGC	Cathode: 0.1 mgcm <sup>-2</sup> , BP: 170kPa, 80 °C, 60%RH	0.697	~0.75	6
LP@PF-2	Cathode: 0.035 mgcm <sup>-2</sup> , BP: 100kPa, 80 °C, 100%RH	~0.8	~0.81	7
PtNi alloy nanocage	Cathode: 0.15 mgcm <sup>-2</sup> , BP: 200kPa, 80 °C, 100%RH	0.92	~1.30	8
Dealloyed PtNi	Cathode: 0.1 mgcm <sup>-2</sup> , BP: 150kPa, 80 °C, 100%RH	~0.9	~1.20	9
Pt67Co31W2	Cathode: 0.11 mgcm <sup>-2</sup> , BP: 150kPa, 80 °C, 100%RH	~0.6	~0.81	10
Dealloyed PtNi/C	Cathode: 0.1 mgcm <sup>-2</sup> , BP: 100kPa, 80 °C, 100%RH	~0.82	1.10	11
Ga-PtNi/C	Cathode: 0.15 mgcm <sup>-2</sup> , BP: 1atom, 65 °C, 100%RH	~0.42	~0.45	12

[a] BP: back pressure

**Table S4.** High-frequency resistance (HFR) values of the MEA at various current densities in H<sub>2</sub>-air fuel cell

Current density / mAcm <sup>-2</sup>	HFR for Pt1Co1-IMC@Pt/C / mΩcm <sup>2</sup>	HFR for PtC / mΩcm <sup>2</sup>
0.05	111.25	104.375
0.1	110	102.5
0.2	108.75	101.25
0.4	106.25	98.75
0.6	104.375	97.5
0.8	101.875	96.875
1	101.25	95.625
1.2	100	95
1.4	98.125	93.75
1.6	95.625	92.5
1.8	95	91.25
2	92.5	89.375
2.2	90.625	87.5
2.4	88.125	85
2.6	85	83.75
2.8	80.625	81.875
3	77.5	80

**Table S5.** High-frequency resistance (HFR) values of the MEA at various current densities in H<sub>2</sub>-O<sub>2</sub> fuel cell.

Current density / mAcm <sup>-2</sup>	HFR for Pt1Co1- IMC@Pt/C / mΩcm <sup>2</sup>	HFR for PtC/ mΩcm <sup>2</sup>
0.1	87.5	85.625
0.2	86.25	85
0.3	85.625	85.625
0.4	85	83.75
0.6	83.75	82.5
0.8	83.125	83.125
1.0	83.75	81.25
1.2	81.875	79.375
1.4	79.375	79.375
1.6	78.125	76.875
1.8	76.875	75.625
2.0	76.875	75
2.2	76.25	76.25
2.4	75	73.75
2.6	73.125	73.75
2.8	70.625	71.875
3.0	68.75	70
3.2	67.5	68.75
3.4	66.875	68.125
3.6	66.25	62.5
3.8	64.375	60.625
4.0	62.5	59.375

## References

1. B.-A. Lu, L.-F. Shen, J. Liu, Q. Zhang, L.-Y. Wan, D. J. Morris, R.-X. Wang, Z.-Y. Zhou, G. Li, T. Sheng, L. Gu, P. Zhang, N. Tian and S.-G. Sun, *ACS Catal.*, 2020, **11**, 355-363.
2. Y. Hu, M. Zhu, X. Luo, G. Wu, T. Chao, Y. Qu, F. Zhou, R. Sun, X. Han, H. Li, B. Jiang, Y. Wu and X. Hong, *Angew. Chem. Int. Ed.*, 2021, **60**, 6533-6538.
3. X. X. Du, Y. He, X. X. Wang and J. N. Wang, *Energy Environ. Sci.*, 2016, **9**, 2623-2632.
4. J. Li, Z. Xi, Y. T. Pan, J. S. Spendelow, P. N. Duchesne, D. Su, Q. Li, C. Yu, Z. Yin, B. Shen, Y. S. Kim, P. Zhang and S. Sun, *J. Am. Chem. Soc.*, 2018, **140**, 2926-2932.

5. X. X. Wang, S. Hwang, Y. T. Pan, K. Chen, Y. He, S. Karakalos, H. Zhang, J. S. Spendelow, D. Su and G. Wu, *Nano Lett.*, 2018, **18**, 4163-4171.
6. W. S. Jung, W. H. Lee, H.-S. Oh and B. N. Popov, *J. Mater. Chem. A*, 2020, **8**, 19833-19842.
7. L. Chong, J. Wen, J. Kubal, F. G. Sen, J. Zou, J. Greeley, M. Chan, H. Barkholtz, W. Ding and D.-J. Liu, *Science*, 2018, **362**, 1276-1281.
8. X. Tian, X. Zhao, Y.-Q. Su, L. Wang, H. Wang, D. Dang, B. Chi, H. Liu, E. J. Hensen and X. W. D. Lou, *Science*, 2019, **366**, 850-856.
9. B. Han, C. E. Carlton, A. Kongkanand, R. S. Kukreja, B. R. Theobald, L. Gan, R. O'Malley, P. Strasser, F. T. Wagner and Y. Shao-Horn, *Energy Environ. Sci.*, 2015, **8**, 258-266.
10. J. Liang, N. Li, Z. Zhao, L. Ma, X. Wang, S. Li, X. Liu, T. Wang, Y. Du, G. Lu, J. Han, Y. Huang, D. Su and Q. Li, *Angew. Chem. Int. Ed.*, 2019, **58**, 15471-15477.
11. F. Dionigi, C. C. Weber, M. Primbs, M. Gocyla, A. M. Bonastre, C. Spori, H. Schmies, E. Hornberger, S. Kuhl, J. Drnec, M. Heggen, J. Sharman, R. E. Dunin-Borkowski and P. Strasser, *Nano Lett.*, 2019, **19**, 6876-6885.
12. J. Lim, H. Shin, M. Kim, H. Lee, K. S. Lee, Y. Kwon, D. Song, S. Oh, H. Kim and E. Cho, *Nano Lett.*, 2018, **18**, 2450-2458.